Bulletin of the Seismological Society of America, 91, 2, pp. 381–396, April 2001

Nonlinear Seismic Effects in Soils: Numerical Simulation and Study

by Olga V. Pavlenko

Abstract To study the effects of nonlinearity in the seismic response of soils, a numerical simulation of the propagation of vertically incident seismic waves in horizontal soil layers were performed. Shear noiselike and monochromatic seismic waves of various intensities were used as input signals. The behavior of soils was described by a nonlinear hysteretic model. To extract and study nonlinear components in the ground response, the nonlinear system identification method and analysis of higher-order spectra of oscillations on the surface were applied. Even for weak input signals, the response of the simulated soils contained a noticeable nonlinear component. An increase in the intensity of input signals led to increasing distortions of propagating signals, due to the generation and growth of combination-frequency harmonics. The results show that odd types of nonlinearity are most typical for soils, such as cubic and fifth-order nonlinearities, causing generation of the third and fifth higher harmonics of main frequencies of input signals. Nonlinearities of even types, such as quadratic, fourth-order, and sixth-order, concerned with asymmetry, or skewness, of oscillations (i.e., quasi-static deformations of the surface) are usually weak, except some special cases, in which a stress-strain relationship of a soil can be represented by functions with noticeable even components. A weak nonlinearity results in an increase in high-frequency components, due to the generation of higher harmonics. In cases of strong nonlinearity, in which a decrease in amplification and in shear moduli become noticeable, changes in spectra of propagating signals achieve their maximum. As a result, input signals with arbitrary spectra are transformed into output signals with spectra of the type of $E(f) \sim f^k$, where k depends on the properties of the medium.

Introduction

The nonlinear behavior of sedimentary soils in strong ground motions remains an unsatisfactorily explored field. In strong earthquakes, we can observe sharp changes in spectral composition and amplitudes of oscillations depending on ground conditions, soil consolidation and sagging, soil loosening and lifting, liquefaction of water-saturated soils, residual deformations, and so on. Overall, the effect is rather complicated and depends on the composition and thickness of soft deposits, on their saturation with water, and on the level of underground water, as well as on the magnitude and frequency content of an earthquake.

At the beginning of the 1970s, laboratory experiments had been performed to study the behavior of soft sediments under loading (Hardin and Drnevich, 1972), and it was found that the stress-strain relationship was hysteretic (Fig. 1a) and that the behavior of sediments was elastic plastic or elastic viscous plastic. Similar relationships were obtained from field experiments with small explosions, in which stress and strain measurements in loam and loess above the level of the underground water were performed simultaneously (Fig. 1b) (Vasil'ev *et al.,* 1969, 1977). Downhole vertical arrays provided further field evidence of nonlinear dynamic soil behavior during earthquakes. Ground motions recorded at the Lotung large-scale seismic test site inferred reduction in shear modulus with increasing effective shear strain, which is found to compare satisfactorily with those obtained through laboratory tests. Nonlinear stress-strain dependencies were obtained directly from the free-field downhole accelerations (Elgamal *et al.,* 1995; Zeghal *et al.,* 1995; Chang *et al.,* 1996).

For a long time, there was a substantial difference in the viewpoints of seismologists and geotechnical engineers on the role of nonlinear wave effects in seismic fields: engineers have been convinced of strong nonlinearities in the behavior of soft soils (at strains smaller than 10^{-4}), while seismologists interpreted strong motion data up to a 0.3–0.4g level with a linear viscoelastic behavior. This discrepancy progressively disappeared with the accumulation of representative experimental data on strong ground motion. Noticeable manifestations of soil nonlinearity were observed in recent earthquakes (Caillot and Bard, 1990; Aki and Irikura, 1991; Darragh and Shakal, 1991; Beresnev *et al.,* 1995;

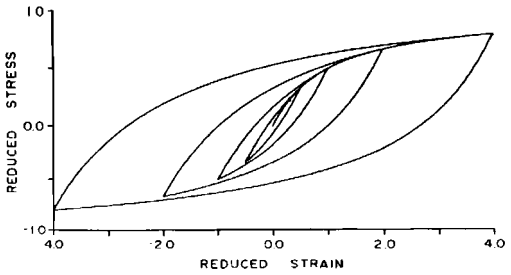

(a)

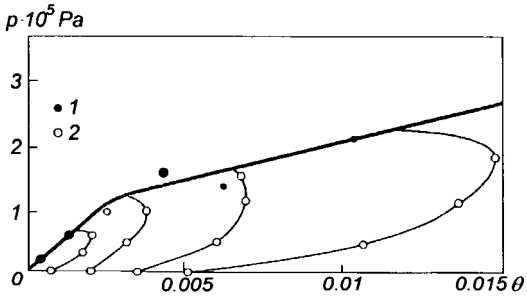

(b)

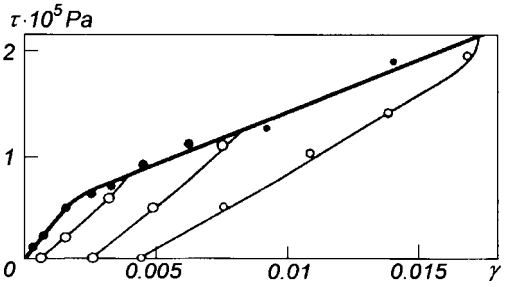

(c)

Figure 1. (a) An initial loading curve of simple shear and hysteresis loops for the elastic-plastic model of soil behavior. Stress and strain are scaled so that the maximum stress and the low-strain modulus are unity, that is, stress is normalized by multiplying by $1/\tau_{max}$, where τ_{max} is the shear stress in failure, and strain is normalized by multiplying by G_{max}/τ_{max}, where G_{max} is the low-strain modulus (derived from Joyner and Chen, 1975). (b) Typical compression and (c) shear stress-strain curves for dry loam in (1) loading and (2) unloading (the natural humidity of 10–15%, $V_p = 300 \div 600$ m/sec, $V_s = 200 \div 250$ m/sec). Field experiments were performed with small explosions, and the relationships were calculated from measurements of the main stress, $\sigma_{ii}(t)$, and strain, $\varepsilon_{ii}(t)$, components in soils near the surface. Normal stresses were measured by small rigid membrane transmitters. Strains were measured by borehole strainmeters with bases of 250–300 mm. Areas of the circles are proportional to the numbers of measurements (Vasil'ev *et al.,* 1977).

Aguirre and Irikura, 1997), and statistical analysis confirmed the tendency toward increasing nonlinearity with increasing intensity of oscillations (Kamiyama, 1992). To describe the nonlinear behavior of soils, various models were constructed with elements of elasticity, plasticity, and viscosity. The conclusion was made that the direction to be followed to bridge the gap between seismologists and geotechnical engineers is the detailed analysis allowed by strong motion data from dense seismic arrays (Bard and Pitilakis, 1995).

In Russia, the nonlinear wave effects in seismic fields have been studied since the 1960s and 1970s (Nikolaev, 1967; Vasil'ev *et al.,* 1969, 1977). First, the purpose was to evaluate nonlinear corrections to the physical characteristics (energy, spectral composition, etc.) of powerful sources of seismic waves (seismic sources, explosions, seismic vibrators), and later to develop new types of receiving and transmitting antenna systems (Gushchin and Shalashov, 1981). The following possible practical applications were proposed based on the determination of nonlinear parameters of sedimentary and crystalline fractured rocks: new methods of seismic microzonation, new sensitive methods of seismic monitoring (based on theoretical and experimental facts that nonlinear parameters are more sensitive to changes in the stress state of the medium than linear parameters), and methods for seismic prospecting (Nikolaev, 1988; Groshkov *et al.,* 1990). Nonlinear seismology developed as a continuation of nonlinear acoustics to seismic frequency bands, and multiple experiments with a vibrator seismic source were performed, aimed at detecting, in seismic fields, the nonlinear effects that had been already found in acoustical fields. Interaction of seismic waves, generation and growth of combination-frequency harmonics, and other nonlinear effects, as well as the influence of dispersion, absorption, and nonlinearity on seismic wave fields, were studied (e.g., Aleshin *et al.,* 1981; Gushchin and Shalashov, 1981; Nikolaev *et al.,* 1995).

The nonlinear phenomena observed in sedimentary soils in strong motions are due to the fact that Hooke's law does not hold for sediments, the stress-strain relationship is nonlinear, that is, its loading and unloading parts can be represented by the power series

$$\sigma(\varepsilon) = a_1\varepsilon + a_2\varepsilon^2 + a_3\varepsilon^3 + a_4\varepsilon^4 + a_5\varepsilon^5 + \ldots, \quad (1)$$

where σ is stress, ε is strain, and a_1, a_2, a_3, a_4, a_5 are constant coefficients. The first term in the series $a_1\varepsilon$ describes the linear dependence (Hooke's law); the others are nonlinear corrections. The nonlinearity of the stress-strain relationship leads to distortions in the shapes of propagating seismic waves; the waves acquire new spectral components. In other words, the waves interact with themselves and with each other in a nonlinear medium, producing new components in their spectra. The quadratic term $a_2\varepsilon^2$ defines the interaction of two waves (for example, at frequencies ω_1 and ω_2) generating combination-frequency harmonics at frequencies $2\omega_1$, $2\omega_2$, $\omega_1 \pm \omega_2$ and the constant component at zero fre-

quency. The cubic term $a_3\varepsilon^3$ defines the interaction of three waves at frequencies ω_1, ω_2, and ω_3 generating combination-frequency harmonics at $3\omega_1$, $3\omega_2$, $3\omega_3$, $\omega_1 + \omega_2 + \omega_3$, $\omega_1 + \omega_2 - \omega_3$, $\omega_1 + 2\omega_2$, $2\omega_1 - \omega_2$, and so forth.

To account for the medium nonlinearity in problems of wave propagation, nonlinear corrections are introduced into wave equations, according to formula (1). By analogy with nonlinear acoustics, it was assumed that the most significant correction to Hooke's law is the quadratic term $a_2\varepsilon^2$, and field experiments performed in Russia were aimed at detecting the quadratic nonlinearity of soils (e.g., Aleshin *et al.,* 1981; Gushchin and Shalashov, 1981; Groshkov *et al.,* 1990; Nikolaev *et al.,* 1995). The assumption of the predominance of quadratic nonlinearity is usually made in studying nonlinear seismic effects (Lund, 1983; Parker, 1988; Dimitrui, 1990). This article shows that soils possess mostly odd types of nonlinearity, that is, the cubic correction to Hooke's law is most sufficient, whereas the quadratic and other even-order terms are less important; however, in some cases even-order terms become comparable with odd-order terms. It should be mentioned that, though field experiments were aimed at detecting even-order higher harmonics, the results often showed a more noticeable increase in harmonics of odd orders (Dimitriu, 1990; Nikolaev *et al.,* 1995).

Though even and odd types of nonlinearity have much in common, they lead to different nonlinear effects. Frequencies of higher harmonics, shapes of seismic solitary waves, and other nonlinear phenomena depend on the type of soil nonlinearity; only even types of nonlinearity are connected with the constant component of the seismic wave field. Preliminary study is required to determine what corrections to the wave equations are most important in one case or another.

In this work, to determine the types and quantitative characteristics of soil nonlinearity, the method of nonlinear system identification was applied, which was successfully used in nonlinear system analysis in many fields of science. A soil with a typical stress-strain relationship was studied to discover general regularities in nonlinear seismic phenomena. This work will be continued by investigation of the nonlinearity of soils in various geotechnical conditions, including their liquefied states. Such work using vertical array records of the 1995 Kobe earthquake is now in preparation.

The issue concerned with the types of soil nonlinearity is closely connected to the problem of generation of higher harmonics of propagating seismic waves. Generation of higher harmonics has not yet been fully explored. Field experiments with a vibrator source were performed without preliminary modeling, accounting for real soil properties, whereas nonlinear models of soil behavior were only applied to calculations of earthquakes and were not used for studying basic nonlinear seismic phenomena. Therefore, another goal of this study is to investigate higher harmonic generation in soils by means of numerical simulation. It is shown that nonlinearity of soil behavior can lead to a certain shape of spectra of propagating signals, in which spectra take the form of $E(f) = f^{-k}$. This is in agreement with the common theory of wave interactions in a nonlinear medium.

Nonlinear System Identification and Higher-Order Spectra and Their Application to the Study of Nonlinearity of Subsurface Soils

The nonlinearity of the seismic response of subsurface soils is determined by their nonlinear stress-strain characteristics, which play the parts of the transfer functions and determine the transformation of input seismic signals into the ground response. Figure 1a, b, and c shows that only the beginning part of this curve, the domain of small deformations, is approximately linear. Therefore, only weak seismic waves keep their shapes in propagating through such media, whereas intense waves suffer distortions. To estimate a ground seismic response at a given point, we should determine the linear and nonlinear domains in the response and compare them with a whole set of possible seismic actions. We should obtain a quantitative description of the ground response to any seismic action. In system analysis this procedure is called nonlinear system identification. The problem of nonlinear system identification is finding such a mathematical description (model) of a system that its seismic response coincides with the response of the real physical system (Marmarelis and Marmarelis, 1978).

To obtain such a description, let us represent our system as a black box with an input and an output. We look for a relation between the input and output signals. In a common case, under the conditions of stationarity, analyticity, and a finite memory of a system (these conditions are usually satisfied for real physical systems), an output signal can be represented as the Volterra series, that is, a sum of multiple integrals of an input signal (Marmarelis and Marmarelis, 1978):

$$\begin{aligned} y(t) = k_0 + \int_0^\infty k_1(\tau)x(t-\tau)d\tau + \\ \int_0^\infty\int_0^\infty k_2(\tau_1,\tau_2)x(t-\tau_1)x(t-\tau_2)d\tau_1 d\tau_2 + \\ + \int_0^\infty\int_0^\infty\int_0^\infty k_3(\tau_1,\tau_2,\tau_3)x(t-\tau_1)x(t-\tau_2)x(t-\tau_3)d\tau_1 d\tau_2 d\tau_3 + \ldots, \end{aligned} \tag{2}$$

where $x(t)$ is an input signal, $y(t)$ is the output signal, t is time, τ, τ_1, τ_2, τ_3 are time delays, and k_0, $k_1(\tau)$, $k_2(\tau_1, \tau_2)$, $k_3(\tau_1, \tau_2, \tau_3)$ are the zero-order, first-order, second-order, and third-order Volterra kernels of the system, which are symmetric functions.

If a system is linear,

$$k_2(\tau_1, \tau_2) = k_3(\tau_1, \tau_2, \tau_3) = \ldots = 0,$$

and knowledge of the first term of the Volterra series (i.e., knowledge of the first-order kernel $k_1(\tau)$, which is the impulse characteristic of the system) is sufficient to describe the system. To describe a nonlinear system, several terms are necessary. The majority of physical systems can be satisfactorily described by the first few terms because the series converges rather quickly. This is stipulated both by the smoothness of the functionals and by a linearizing effect of noise (noise accompanying measurements as well as noise occurring inside the system).

The Wiener series is widely used along with the Volterra series. It consists of functionals, which are linear combinations of functionals of the Volterra type. Terms in the Wiener series are orthogonal with respect to the input signal in the form of the Gaussian white noise, so we can determine the Wiener kernels independently from each other. From the other side, the Gaussian white noise as an input signal allows the most effective testing of the system because the Gaussian white noise is a very rich signal: it contains components of all frequencies and amplitudes. Thus, the determination of the Wiener kernels of a system is a good method for its identification (Marmarelis and Marmarelis, 1978). In this case, the dependence of the system response upon an input signal can be written in the form:

$$y(t) = \sum_{m=0}^{\infty} G_m[h_m(\tau_1, \ldots, \tau_m);\ x(t'),\ t' \le t], \quad (3)$$

where G_m are orthogonal functionals, if $x(t)$ is the Gaussian white noise with a zero mean, $\{h_m(\tau_1, \ldots, \tau_m)\}$ is the sequence of the Wiener kernels, and $\tau_1, \ldots, \tau_m$ are time delays. Each kernel is a symmetric function. The first four Wiener functionals are represented in the form:

$$G_0[h_0;\ x(t)] = h_0, \quad (4)$$

$$G_1[h_1;\ x(t)] = \int_0^{\infty} h_1(\tau)x(t-\tau)d\tau, \quad (5)$$

$$G_2[h_2;\ x(t)] = \int_0^{\infty}\int h_2(\tau_1,\tau_2)x(t-\tau_1)x(t-\tau_2)d\tau_1 d\tau_2 - P\int_0^{\infty} h_2(\tau_1,\tau_1)d\tau_1, \quad (6)$$

$$G_3[h_3;\ x(t)] = \int_0^{\infty}\int\int h_3(\tau_1,\tau_2,\tau_3)x(t-\tau_1)x(t-\tau_2)x(t-\tau_3)d\tau_1 d\tau_2 d\tau_3 - 3P\int_0^{\infty}\int h_3(\tau_1,\tau_2,\tau_2)x(t-\tau_1)d\tau_1 d\tau_2, \quad (7)$$

where τ is time delay, P is the intensity of the white noise not depending on frequency.

Orthogonality of terms in the Wiener series with respect to the Gaussian white noise provides essential advantages in describing nonlinear systems: (1) effective methods can be used in estimating kernels, based on determination of cross-correlation functions; and (2) limited numbers of these terms can represent the best approximations for a real system from the viewpoint of the minimal mean square error. By analogy with an ordinary impulse characteristic $h(t)$, kernel series $\{h_m\}$ can be treated as a generalized, composed impulse characteristic of a system. The first-order kernel determines the linear part of the system response, whereas higher-order kernels describe the interactions between the values of the input signal in the past with respect to their influence on the response at present (Marmarelis and Marmarelis, 1978).

In this study, the kernels of the system were found by the cross-correlation method described in (Marmarelis and Marmarelis, 1978). The zero-order kernel is equal to the average of the response of the system to the Gaussian white noise:

$$h_0 = E[y(t)]. \quad (8)$$

The first-order kernel is expressed through the cross-correlation function of the input white noise and the response of the system:

$$h_1(\tau) = (1/P)E[y(t)x(t - \tau)]. \quad (9)$$

The second-order kernel is defined as

$$h_2(\tau_1, \tau_2) = (1/2P^2)E[y_1(t)x(t - \tau_1)x(t - \tau_2)], \quad (10)$$

where

$$y_1(t) = y(t) - G_1[h_1, x(t)] - G_0[h_0, x(t)], \quad (11)$$

and the third-order kernel is

$$h_3(\tau_1, \tau_2, \tau_3) = (1/6P^3)E[y_2(t)x(t - \tau_1)x(t - \tau_2)x(t - \tau_3)], \quad (12)$$

where

$$y_2(t) = y(t) - G_2[h_2, x(t)] - G_1[h_1, x(t)] - G_0[h_1, x(t)] \quad (13)$$

(Marmarelis and Marmarelis, 1978).

The mean square error of approximation is a quantitative measure of the agreement between the model and the real system response. The constant component of the response corresponding to the zero-order kernel $\{h_0\}$ gives a zero-approximation error. The mean square deviation of the

response from this line is calculated and normalized so that it is 100. Then the mean square deviation is estimated from the response from the model $\{h_0, h_1\}$, which uses the first-order kernel, and is normalized by the same value as was previously normalized for the zero-approximation error. The deviations then are calculated and normalized by the same value of the real system response from responses of the nonlinear models predicted by the kernels $\{h_0, h_1, h_2\}$ and $\{h_0, h_1, h_2, h_3\}$ (Marmarelis and Marmarelis, 1978). Performing these calculations, we estimate the degree to which the second-order $\{h_2\}$ and the third-order $\{h_3\}$ kernels contribute to the nonlinear component of the system response, and we draw conclusions regarding the types and quantitative characteristics of the system nonlinearity. If the second-order kernel $\{h_2\}$ gives the largest contribution, the system possesses mostly quadratic nonlinearity; if the third-order kernel $\{h_3\}$ contributes more, the system is cubic-nonlinear, etc. The system is virtually linear, if nonlinear components in the response are negligibly small.

In spectral terms, the response of a nonlinear system can be represented by the sequence of spectra: the power spectrum, bispectrum, trispectrum, and other higher-order spectra (Marmarelis and Marmarelis, 1978; Nikias and Raghuveer, 1987). The Nth-order spectrum $C_N(\omega_1, \omega_2, \ldots, \omega_{N-1})$ of the real discrete stationary process $x(k)$ is defined as the Fourier transform of its Nth-order cumulant sequence $c_N(\tau_1, \tau_2, \ldots \tau_{N-1})$, i.e.,

$$C_N(\omega_1, \omega_2, \ldots, \omega_{N-1}) = \sum_{\tau_1=-\infty}^{\infty} \cdots \sum_{\tau_{N-1}=-\infty}^{\infty} c_N(\tau_1, \tau_2, \ldots, \tau_{N-1}) \cdot \exp\{-j(\omega_1\tau_1 + \ldots + \omega_{N-1}\tau_{N-1})\} \quad (14)$$

(Nikias and Raghuveer, 1987). The power spectrum, bispectrum, and trispectrum are special cases of the Nth-order spectrum, i.e., power spectrum ($N = 2$):

$$C_2(\omega_1) = \sum_{\tau_1=-\infty}^{\infty+} c_2(\tau_1) \exp\{-j(\omega_1\tau_1)\}, \quad (15)$$

bispectrum ($N = 3$):

$$C_3(\omega_1, \omega_2) = \sum_{m=-\infty}^{+\infty} \sum_{n=-\infty}^{+\infty} c_3(\tau_1, \tau_2) \exp\{-j(\omega_1\tau_1 + \omega_2\tau_2)\}, \quad (16)$$

trispectrum ($N = 4$):

$$C_4(\omega_1, \omega_2, \omega_3) = \sum_{\tau_1=-\infty}^{\infty} \sum_{\tau_2=-\infty}^{\infty} \sum_{\tau_3=-\infty}^{\infty} c_4(\tau_1, \tau_2, \tau_3) \cdot \exp\{-j(\omega_1\tau_1 + \omega_2\tau_2 + \omega_3\tau_3)\}. \quad (17)$$

Here $c_2(\tau_1)$, $c_3(\tau_1, \tau_2)$, and $c_4(\tau_1, \tau_2, \tau_3)$ are sequences of the second-order, third-order, and fourth-order cumulants of the process $x(k)$, respectively. While the second-order and third-order cumulants and the second-order and third-order moments are identical:

$$c_2(\tau_1) = m_2(\tau_1) = E[x(k)x(k+\tau_1)], \quad (18)$$

$$c_3(\tau_1,\tau_2) = m_3(\tau_1, \tau_2) = E[x(k)x(k+\tau_1)x(k+\tau_2)], \quad (19)$$

(where $E[\ ]$ means averaging), this is not true for the fourth-order (and higher) statistics. To generate the fourth-order (and higher) cumulant sequence, we need to know the moment and autocorrelation sequences.

Analysis of higher-order spectra of signals passing through a nonlinear system also allows determination of the types and quantitative parameters of the nonlinearity of the system (Nikias and Raghuveer, 1987).

In this work, normalized higher-order spectra, that is, higher-order coherences are estimated. One-dimensional diagonal ($\omega_1 = \omega_2 = \ldots = \omega_{N-1} = \omega$) fourth-, fifth-, and sixth-order coherences are constructed by analogy with the bicoherence $r_3^2(\omega_1, \omega_2)$ (Haubrich, 1965):

$$r_3^2(\omega_1, \omega_2) = \frac{|C_3(\omega_1, \omega_2)|^2}{C_2(\omega_1)C_2(\omega_2)C_2(\omega_1 + \omega_2)}. \quad (20)$$

The fourth-order coherence (tricoherence) is calculated by the equation

$$r_4^2(\omega) = \frac{|C_4(\omega)|^2}{C_2^3(\omega)C_2(3\omega)}, \quad (21)$$

the fifth-order coherence is calculated by the equation

$$r_5^2(\omega) = \frac{|C_5(\omega)|^2}{C_2^4(\omega)C_2(4\omega)}, \quad (22)$$

and the sixth-order coherence is calculated by the equation

$$r_6^2(\omega) = \frac{|C_6(\omega)|^2}{C_2^5(\omega)C_2(5\omega)}. \quad (23)$$

Higher-order coherences take values from 0 to 1 and have a simple physical meaning, which can be explained by the following example. Let a signal at the input of a system with quadratic (or cubic) nonlinearity contain, among others, oscillations at frequencies ω_1 and ω_2. Then the output signal will contain oscillations at frequencies ω_1, ω_2, as well as at combination frequencies $2\omega_1$, $2\omega_2$, $\omega_1 + \omega_2$, and $\omega_1 - \omega_2$ (in the case of cubic nonlinearity, $3\omega_1$, $3\omega_2$, $\omega_1 + \omega_1 + \omega_2$, $\omega_1 + \omega_2 + \omega_2$, $\omega_1 + \omega_1 - \omega_2$, etc.), the phases of these signals are connected by certain relations called quadratic (cubic) phase coupling. For two given frequencies, ω_1 and ω_2, bicoherence $r_3^2(\omega_1, \omega_2)$ is equal to the part of the power

spectral density at frequency $\omega_1 + \omega_2$, which is coupled with harmonics at frequencies ω_1 and ω_2. For three given frequencies ω_1, ω_2 and ω_3, respectively, tricoherence $r_4^2(\omega_1, \omega_2, \omega_3)$ is the part of the power spectral density at frequency $\omega_1 + \omega_2 + \omega_3$, coupled with harmonics ω_1, ω_2, and ω_3. If the values of higher-order coherence $r_N^2(\omega_1, \omega_2, \ldots, \omega_{N-1})$ are close to 1, a high phase coherence takes place. Therefore, the combination-frequency harmonic $\omega_1 + \omega_2 + \ldots + \omega_{N-1}$ is the result of the interaction of the main harmonics $\omega_1, \omega_2, \ldots, \omega_{N-1}$. On the other side, if the values are close to 0, the harmonics $\omega_1, \omega_2, \ldots, \omega_{N-1}$ and $\omega_1 + \omega_2 + \ldots + \omega_{N-1}$ are independent.

In the considered example, the generation of harmonics at frequencies $2\omega_1$, $2\omega_2$, $\omega_1 + \omega_2$, and $\omega_1 - \omega_2$ proceeds simultaneously as a common process, and the knowledge of one of these processes (for example, generation of harmonic $\omega_1 + \omega_2$) is sufficient for getting a representation of the nonlinearity of the system and of other processes. Respectively, higher-order spectra possess symmetry properties, and their different symmetric regions correspond to these different harmonics. Knowledge of a higher-order spectrum in one of its symmetric regions (for example, knowledge of the bispectrum in the triangular region $\omega_2 \geq 0$, $\omega_1 \geq \omega_2$, $\omega_1 + \omega_2 \leq \pi$) is enough for its complete description (Nikias and Raghuveer, 1987), as well as for getting a representation of nonlinear interactions in the medium. A special case is the generation of harmonics at frequencies $2\omega_1$ and $2\omega_2$, which correspond to diagonal values of higher-order spectra. Without essential loss of information, we can use the more descriptive one-dimensional higher-order spectra instead of clumsy multidimensional higher-order spectra to get a representation of the nonlinearity of the system.

In this work, conventional direct methods for higher-order spectral estimation were used based on fast Fourier transform (FFT), which gave nonbiased and consistent estimates. To estimate higher-order spectra for the sequence $x(k)$, the sequence is divided into p equal nonoverlapping intervals, over which averaging of estimates is performed. Estimates become smooth for sufficiently large p (Nikias and Raghuveer, 1987). If $x(k)$ is a stationary Gaussian process, for large p, bicoherence values $r_3^2(\omega_1, \omega_2)$ are approximately χ^2 distributed with 2 degrees of freedom and the expected mean value of $\sim 1/p$ for nondiagonal terms (Haubrich, 1965). It can be easily shown that bicoherence, tricoherence, fifth-order coherence, and sixth-order coherence values are approximately χ^2 distributed with 2 degrees of freedom, and the expected mean value of $\sim (N-1)!/p$ for diagonal terms, where N is the order of the coherence, and the multiplier $(N-1)!$ appear because of the symmetry properties of higher-order spectra. For a Gaussian process, which passed through a nonlinear system, mean values of higher-order coherence are larger than $(N-1)!/p$. In this case, high values of bicoherence testify to the quadratic nonlinearity of the system and give its quantitative estimates. High values of tricoherence (or the fifth- and sixth-order coherences) testify to the cubic (or fifth- and sixth-order) nonlinearity of the system and give its quantitative estimates. Thus, we determine the types and quantitative parameters of the system nonlinearity.

In engineering seismology, the propagation of a vertically incident seismic wave in horizontally layered sediments is also a problem of the transformation of the seismic wave by a nonlinear system. Here, the input signal is the incident seismic wave, and the output signal is the movement on the surface. In this work, numerical simulation was performed, and the movement on the surface was calculated for the input signals of three types: the Gaussian white noise, monochromatic signals, and sums of two monochromatic signals. First, the system was tested by the Gaussian white noise, and the Wiener kernels were calculated by the method of cross-correlation functions (Marmarelis and Marmarelis, 1978); linear parts of the ground response and nonlinear corrections were determined. Then monochromatic signals at frequencies of 2, 5, 8, 11, 14, and 17 Hz and pairs of these signals were used as input signals, and their nonlinear distortions in the medium were studied. Input signals of various intensities were used to establish regularities in nonlinear seismic processes in soils.

To calculate oscillations on the surface, an algorithm was used elaborated by Joyner and Chen (implicit method, Joyner and Chen, 1975), in which the rheological nonlinear elastic-plastic Iwan model was applied, which is similar to that obtained in laboratory experiments by Hardin and Drnevich (1972). Hysteresis loops shown in Figure 1a correspond to this model. The accuracy of the modeling depends upon the number n of elements used. Calculations were performed for $n = 50$ as in the original article (Joyner and Chen, 1975). This algorithm implies the stress-strain relationship to be a transfer function of the medium, which was very satisfactory for the purposes of this study.

The soil profile used in the numerical simulation was the same as in the article by Joyner and Chen (1975): a horizontally layered sedimentary column bounded above by the free surface and below by a semi-infinite elastic medium representing the bedrock. The same normalized curves shown in Figure 1a were used for all of the soil layers; differences in soil behavior from one layer to another resulted from differences in the values of shear stress in failure τ_{max} and the low-strain shear modulus G_{max} assigned to different layers. The soil profile was a 200-m section of firm alluvium with a density of 2.05 g/cm^3. Shear stress in failure, τ_{max}, and the S-wave velocity progressively increased with depth. Parameters of the underlying half-space were the same as in the article by Joyner and Chen: the substratum was assigned a shear velocity of 2.0 km/sec, and a density of 2.6 g/cm^3; part of the energy of the incident wave was radiated back into the underlying medium.

The choice of the nonlinear model depended on a few factors. On the one hand, this model captured common elements of nonlinear soil behavior that made it useful for a baseline evaluation of site response. On the other hand, it was simple, and therefore it was advantageous for studying

new phenomena. In the study presented here, the complexity of the model could be a nuisance, and it is shown below that the obtained conclusions are of a rather common character. The choice of the nonlinear model influences quantitative characteristics of nonlinearity, but cannot add anything qualitatively new to the results. The same can be said about the site geometry. Only quantitative estimates are influenced by the site geometry. According to the theory of wave propagation in a nonlinear medium, nonlinear distortions are accumulated, therefore, the thicker the sedimentary layer, the more pronounced the manifestations of nonlinearity (Zarembo and Krasil'nikov, 1966).

Results and Discussion

Figure 2a, b, and c represents examples of the response of the studied system of soil layers to the Gaussian noise in a wide frequency range (0.3–170 Hz), obtained in numerical simulation and predicted by models. Estimates of the zero-, first-, second-, and third-order kernels of the system were based on input and output signals of 65,000 points of duration (190 sec).

Zero-order kernels h_0 are constant components of the seismic wave field at the surface, namely, the quasi-static deformations of the surface. They are small, but nonzero; for different time intervals of the response they take positive or negative values, which are larger for higher-intensity input signals. The limits of their variations are approximately proportional to the mean square amplitudes $\langle V^2(t)\rangle$ of oscillations on the surface, which is in agreement with the theory of nonlinear wave interactions (Zarembo and Krasil'nikov, 1966), and they are presented in Table 1. This means that horizontal displacements of points on the surface in positive and negative directions are different, that is, subsurface layers slowly shift to one or the other side in their oscillations. This effect can be interpreted as a result of accumulation of residual shift deformations on the surface. Asymmetry, skewness of oscillations, is concerned with even nonlinearities, which were fairly small in this case, considering the small values of h_0.

First-order kernels $h_1(\tau)$ were estimated in 300 points, two-dimensional second-order kernels $h_2(\tau_1, \tau_2)$ were estimated in 7225 points, and three-dimensional third-order kernels $h_3(\tau_1, \tau_2, \tau_3)$ were estimated in 125,000 points. Based on these kernels, the response of the linear model (Fig. 2a–c, trace 3) and nonlinear corrections accounting for quadratic (Fig. 2a–c, trace 5) and cubic (Fig. 2a–c, trace 7) nonlinearities were constructed according to equations (3) to (7). Trace 4 (Fig. 2a–c) represents the deviation of the real system response from the response of the linear model constructed by the zero- and first-order kernels $\{h_0, h_1\}$. Trace 6 (Fig. 2a–c) is the deviation of the system response from the response of the nonlinear model predicted by kernels $\{h_0, h_1, h_2\}$. Trace 8 (Fig. 2a–c) is the deviation of the system response from the response of the nonlinear model predicted by kernels $\{h_0, h_1, h_2, h_3\}$. For the studied system, considering quadratic and cubic nonlinearities decreases the mean square error of approximation as is shown in Table 1.

Progressive decrease in the mean square error showed that the system is substantially nonlinear, and the second- and third-order kernels considerably improved the system's description. Accounting for quadratic nonlinearity decreased the mean square error only by ~2%, whereas accounting for cubic nonlinearity decreased it by 6–10%, that is, the system possessed a weak quadratic nonlinearity and a substantial cubic nonlinearity. Note that the intensity of the quadratic and cubic nonlinear components increases with the increasing intensity of the input signal.

A fairly large residual remained after subtracting the linear component and the corrections due to the quadratic and cubic nonlinearities from the calculated system response. The residual can be related to the influence of the higher-order (fourth-order, fifth-order, etc.) nonlinearities, as well as to inaccuracies in estimating kernels. These inaccuracies are caused by various reasons, such as the finite duration and the boundedness of the spectral band of the Gaussian noise, truncation of the tails of normal distribution of noise amplitudes, and inaccuracies in calculations (the detailed error analysis and correction methods are given in Marmarelis and Marmarelis, 1978).

Analyzing changes in shapes and spectra of seismic waves (Fig. 3a–c), three cases are considered: (a) the input signal is monochromatic, (b) it is a sum of two monochromatic signals, and (c) it is the Gaussian noise in a wide frequency range (0.3–170 Hz). The first row of seismograms (1) is the input signal, the second row shows the oscillations on the surface for four different intensities of input signals corresponding to those listed in Table 1, and the bottom row (8) shows the respective stress-strain curves. Increase in amplitudes of input signals shifts working intervals of the curves to nonlinear domains, which induces nonlinear distortions: changes in amplification and spectral composition of signals and acquisition of high-frequency and low-frequency combination harmonics, namely, nonlinear effects (Zarembo and Krasil'nikov, 1966).

For a nonlinear system, the spectrum of the output signal always differs from the spectrum of the input signal; usually, it is more complicated. Changes in the spectral composition of signals are shown in row (3) in Figure 3a–c. Input signal spectra are shown with thin lines, and corresponding spectra of output signals on the surface are shown with thick lines. Given that the input signal is monochromatic, its nonlinear distortions are due to generation and growth of the third, fifth, seventh, and so on, harmonics of the main frequency (Fig. 3a: higher harmonics at frequencies of 15, 25, 35, 45, and 55 Hz); therefore, we can conclude that the system possessed odd types of nonlinearity.

The richer the spectrum of the input signal is, the more complicated the spectrum of the response of a nonlinear system is, which is a result of wave interactions that are more diverse. The superposition principle is not satisfied in a nonlinear system; the system response to a sum of two signals

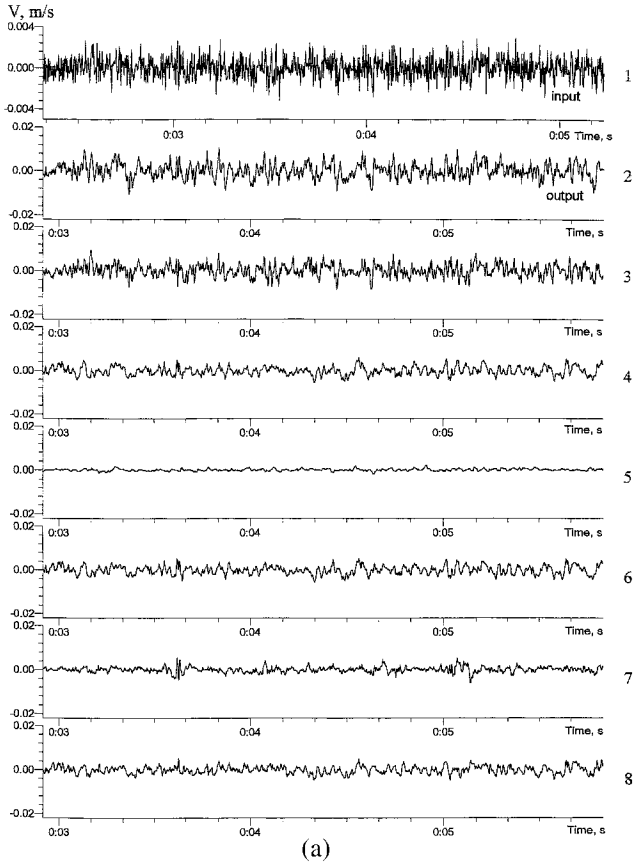

(a)

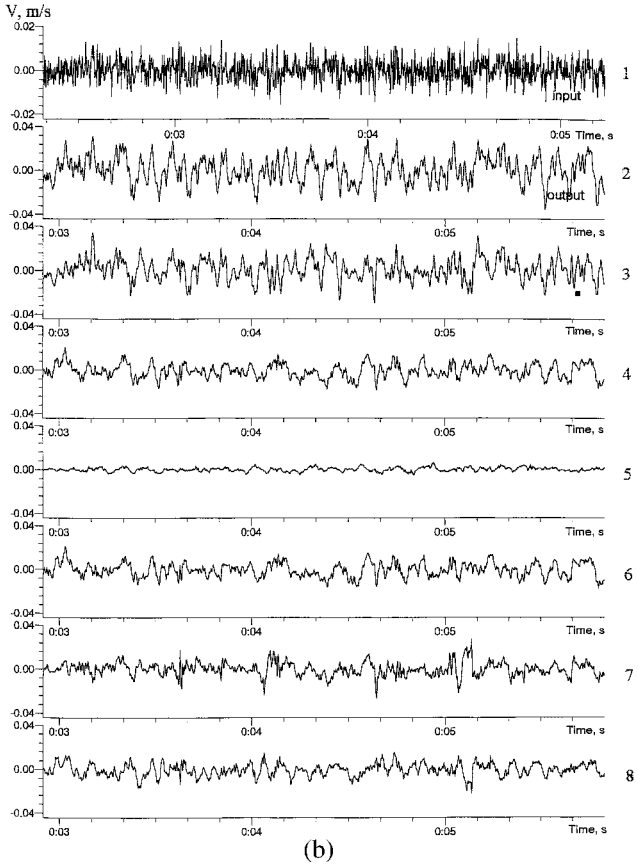

(b)

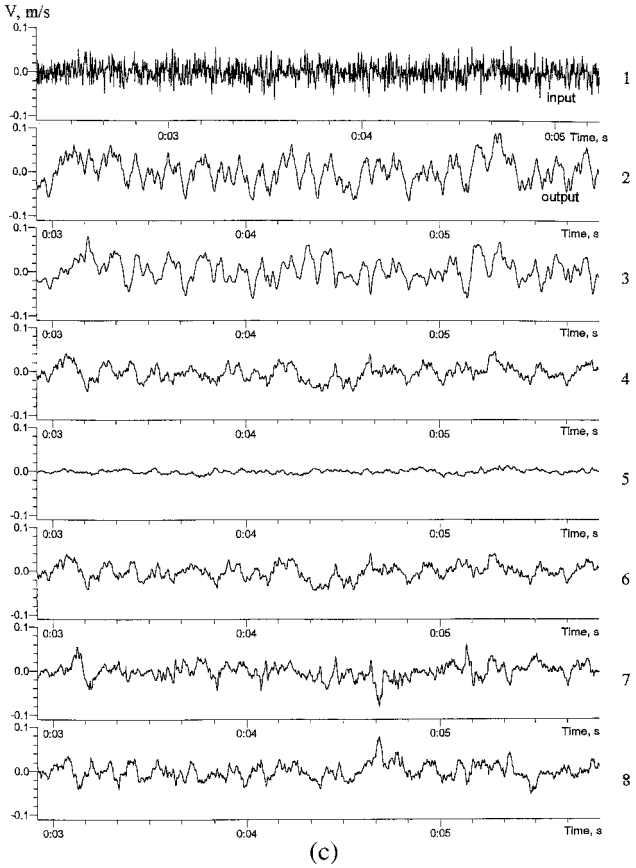

(c)

Figure 2. The response of the system of soil layers to the Gaussian white noise of various intensities: (a) $-\sqrt{\langle V^2(t)\rangle} =$ 0.001 m/sec, (b) $-\sqrt{\langle V^2(t)\rangle} = 0.005$ m/sec, (c) $-\sqrt{\langle V^2(t)\rangle} = 0.02$ m/sec. 1 is the input signal; 2 is the response of the system; 3 is the response predicted by a linear model; 4 is the difference between the response of the system and the response predicted by a linear model; 5 is the nonlinear correction due to quadratic nonlinearity predicted by kernel $\{h_2\}$; 6 is the difference between the response of the system and the response predicted by the model $\{h_0, h_1, h_2\}$; 7 is the nonlinear correction due to cubic nonlinearity predicted by kernel $\{h_3\}$; 8 is the difference between the response of the system and the response predicted by the model $\{h_0, h_1, h_2, h_3\}$.

Table 1
Limiting Values of h_0 and Mean Square Errors of Approximation

Intensity $\sqrt{\langle V^2(t)\rangle}$ (m/sec)			Mean Square Errors for Models			
Input Signal	Output Signal	Limiting h_0 (m/sec)	$\{h_0\}$	$\{h_0, h_1\}$	$\{h_0, h_1, h_2\}$	$\{h_0, h_1, h_2, h_3\}$
0.001	0.003	10^{-6}	100	32.4	30.4	25.6
0.005	0.01	10^{-5}	100	33.8	32.5	26.7
0.02	0.03	10^{-4}	100	41.4	38.9	33.2
0.1	0.1	10^{-3}	100	56.7	54.0	43.3

differs from a sum of the responses to each of these signals. If an input signal is a sum of two harmonics, for example, at frequencies of 5 and 11 Hz (Fig. 3b), its propagation in a nonlinear medium is accompanied by the generation of higher third, fifth, seventh, and so on, harmonics of each of these frequencies: 15, 25, 35, 45, 33, 55 Hz, etc., as well as by the generation of combination-frequency harmonics of 21 Hz (5 + 5 + 11 Hz), 27 Hz (5 + 11 + 11 Hz), 17 Hz (11 + 11 − 5 Hz), 37 Hz (5 + 5 + 5 + 11 + 11 Hz), 43 Hz (5 + 5 + 11 + 11 + 11 Hz), 39 Hz (11 + 11 + 11 + 11 − 5 Hz), 49 Hz (11 + 11 + 11 + 11 + 5 Hz), and many other combination-frequency harmonics of the fifth, seventh, and so on, orders as a result of higher-order interactions. At the same time, combination-frequency harmonics, evidently indicating even types of nonlinearity, are absent in the spectra of output signals.

Generation of combination-frequency harmonics leads to redistribution of energy between spectral components. For rather intense input seismic signals, the power spectral density of oscillations on the surface takes the form of $E(f) \sim f^{-k}$ (where f is frequency and k depends on the properties of the medium), regardless of the spectral composition of an input signal (Fig. 3a–c, the last columns). A similar dependence was derived theoretically in nonlinear acoustics. Nonlinear wave effects in the acoustic field cause redistribution of energy over the spectrum. In the case of the interaction of a large number of waves, the power spectral density of the resulting field is characterized by the dependence of $E(f) \sim f^{-2}$, provided that the medium is nondispersive and does not contain sources and absorbers of energy (Kadomtsev and Karpman, 1971). Dispersion and absorption hinder the development of nonlinear processes, that is, dispersion impedes the transition of energy of the main-frequency harmonic to its higher harmonics, whereas absorption leads to a quicker attenuation of higher harmonics. Therefore, coefficient k depends on dispersion, absorption, and nonlinear properties of the medium.

Therefore, the results of the simulation show that generation of combination-frequency harmonics is observed even for small amplitudes of input signals, whereas other nonlinear effects, such as decrease in amplification and decrease in the shear modulus, become noticeable only for rather large input signals, when changes in the spectra of propagating signals achieve their maximum (Fig. 3a–c, rows 2, 3, and 8). Fig. 3a–c, row 8 represents the working areas of stress-strain curves for various input signals. These figures show that decrease in amplification and decrease in the shear modulus are not noticeable for small amplitudes of input signals.

Based on the results of the simulation, we concluded that increase in high-frequency components is expected in cases of weak nonlinearity (i.e., weak input signals and/or thin sedimentary deposit) but is not expected in cases of strong nonlinearity (i.e., strong input signals and/or thick layer of sediments). In the latter case, input signals with any arbitrary spectra will be transformed into output signals on the surface with spectra of the type of $E(f) \sim f^{-k}$, where k depends on the properties of the medium. A demonstrative example of such spectral changes are the acceleration records of the 1995 Kobe earthquake at Port Island downhole group, where high-frequency spectral components are decreasing and low-frequency components are increasing in accelerogramms from the depth to the surface (Aguirre and Irikura, 1997).

Power spectra and higher-order coherences of input and output signals characterize quantitatively nonlinear distortions of signals in the medium. Figure 3a–c represents bicoherence $r_3^2(\omega)$ (row 4), tricoherence $r_4^2(\omega)$ (row 5), fifth-order coherence $r_5^2(\omega)$ (row 6), and sixth-order coherence $r_6^2(\omega)$ (row 7). Thin lines correspond to the higher-order characteristics of input signals, and thick lines correspond to those for surface oscillations.

Figure 3a, b, and c (rows 4, 5, 6, and 7) show that increase in the intensity of input signals leads to increase in tricoherence and the sixth-order coherence of signals on the surface. If an input signal is monochromatic or a sum of monochromatic signals (Fig. 3a, b), increase in the fourth- and sixth-order coherences at the main frequencies of the input signal (i.e., at 5 Hz and 11 Hz) indicates the generation of their third and fifth higher harmonics. For input signal amplitudes that are rather high, the fourth- and sixth-order coherences are close to 1 at the main frequencies of input signals (5 Hz—Fig. 3a; 5 Hz and 11 Hz—Fig. 3b). This means that an entire phase coupling occurs between the main frequency and its third and fifth harmonics.

The results show that the generation of higher harmonics is more effective for higher main frequencies (i.e., more effective for frequency 11 Hz than for 5 Hz, Fig. 3b). As was mentioned previously, propagation of monochromatic signals at frequencies of 2, 5, 8, 11, 14, and 17 Hz was studied, and although working intervals of the stress-strain diagrams were similar, the third and fifth harmonics were generated most effectively for the input signal at frequency 17 Hz. This is in agreement with the theory of nonlinear wave interactions: amplitudes of combination-frequency harmonics are proportional to their wave numbers, that is, higher-frequency combination harmonics are generated more effectively than lower-frequency ones (Zarembo and Krasil'nikov, 1966). The conclusion of a more effective generation of higher harmonics for higher frequencies of input signals, as well as the alternative sign of quasi-static shift

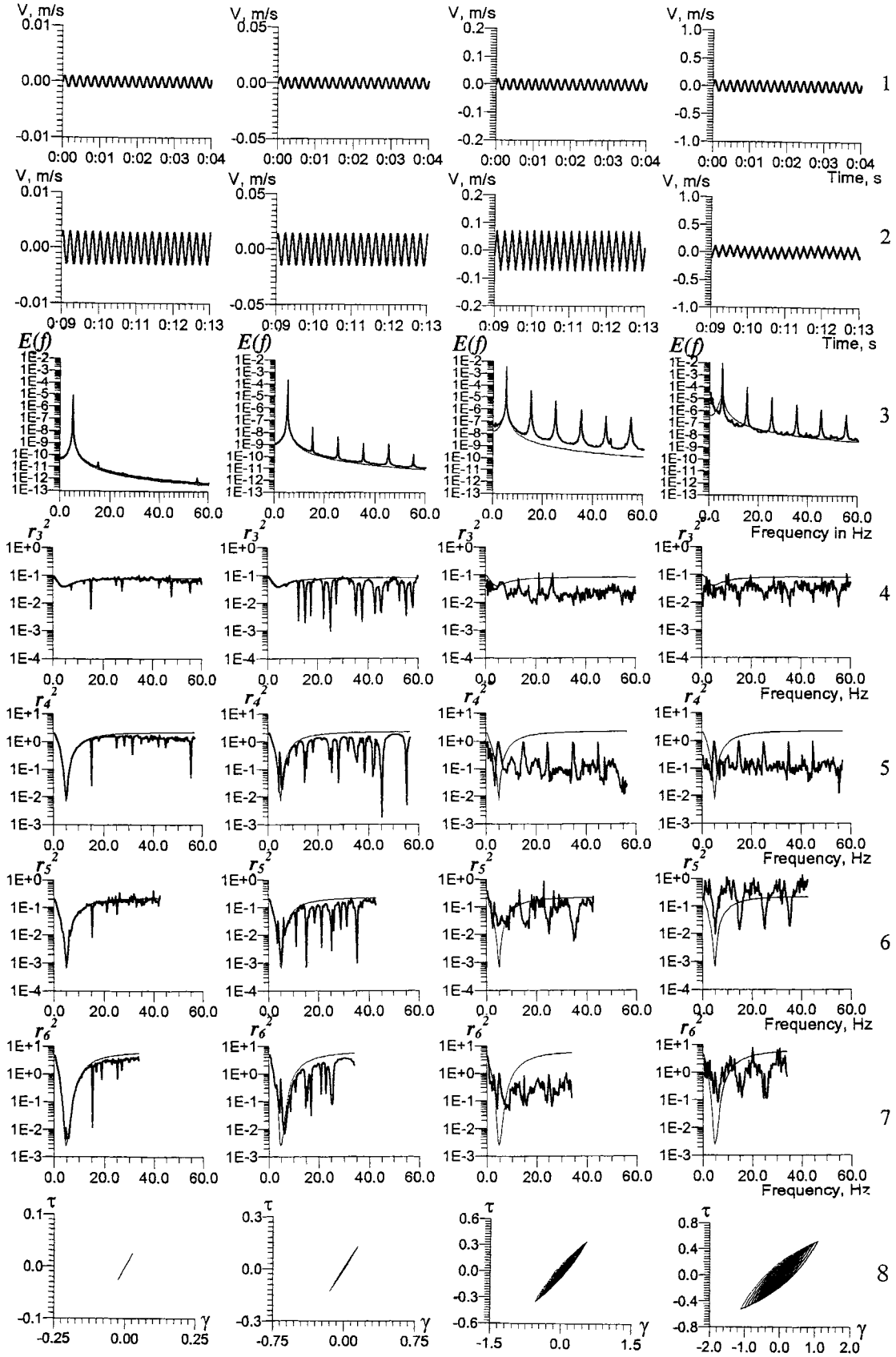

(a)

Figure 3. *Caption on page 393.*

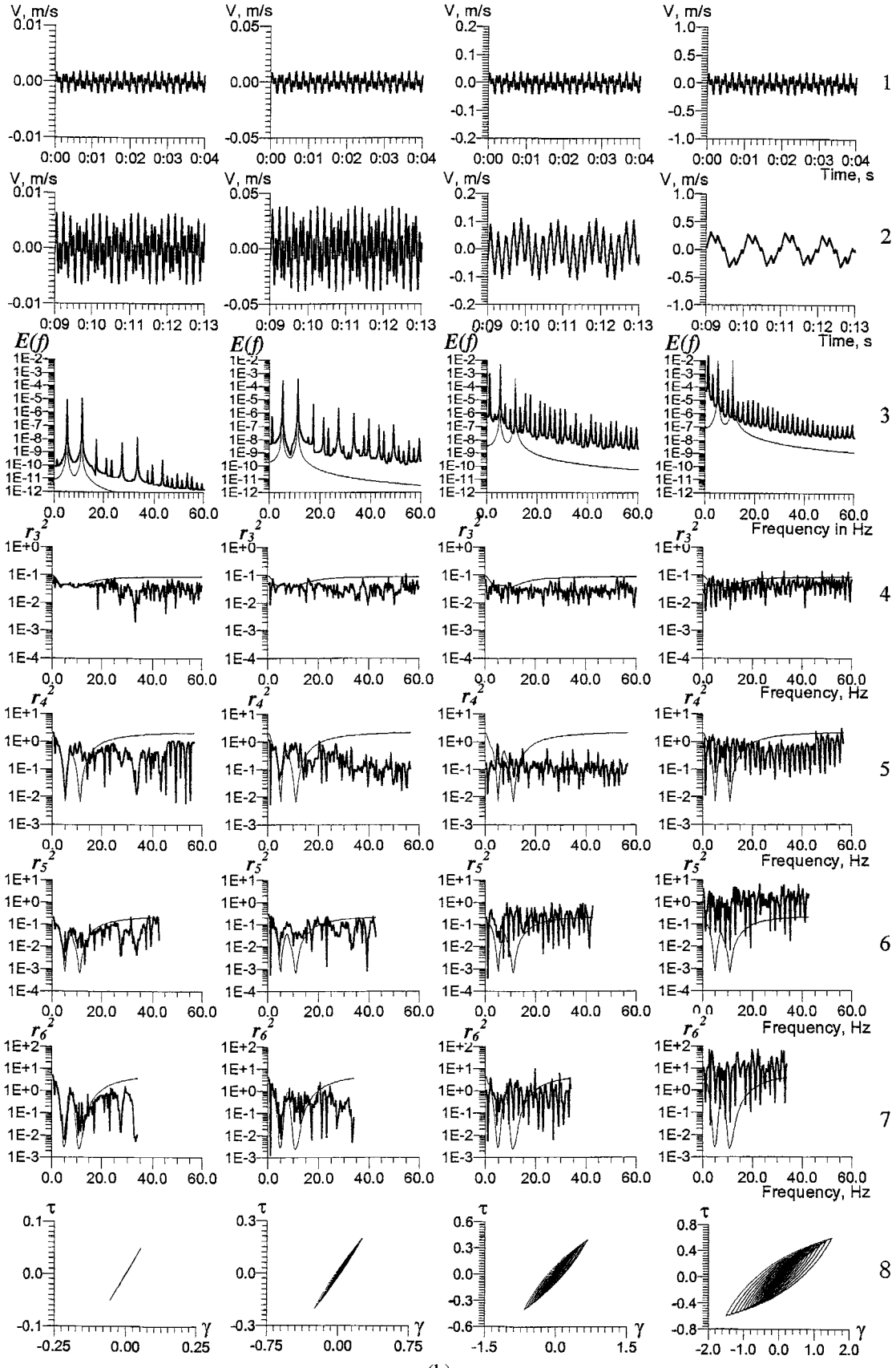

(b)

Figure 3. *(Continued).*

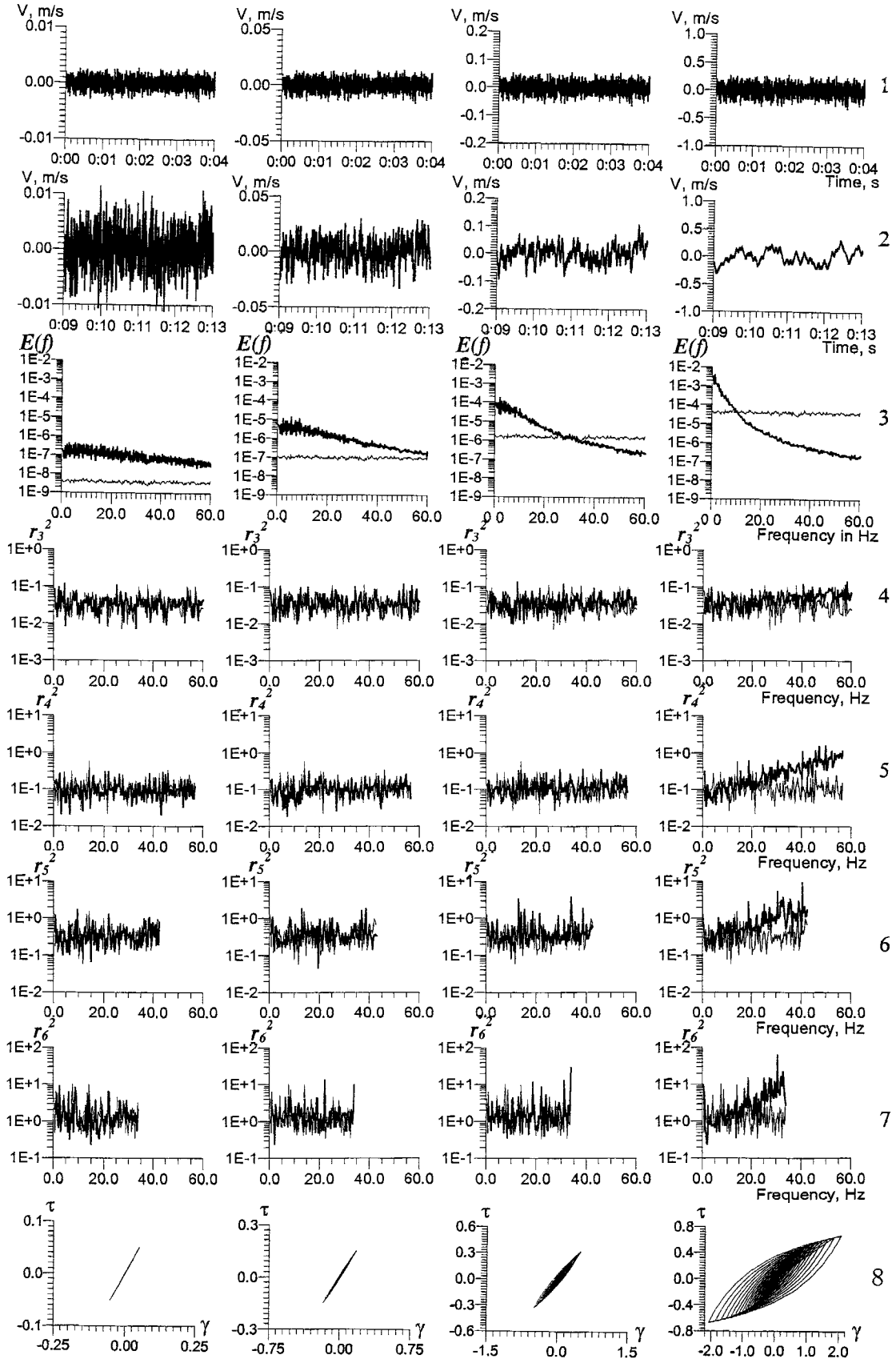

(c)

Figure 3. *(Continued).*

deformations on the surface, agree with the results described in Zvolinskii (1982), in which the propagation of a sinusoidal wave in an elastic or plastic layer was calculated. Positive and negative quasi-static deformations of the surface were measured in field experiments with a vibrator seismic source at distances of hundreds of meters from the vibrator (Nikolaev *et al.,* 1995).

If amplitudes of an input sinusoidal signal are rather high, its propagation in a nonlinear medium is accompanied by large distortions; the number of combination-frequency harmonics is high, and the signal becomes noiselike (Fig. 3a,b, last columns). The power spectral density takes the form of $E(f) \sim f^{-k}$, and the mean values of higher-order coherences approach the value of $(N-1)!/p$, which is characteristic for noiselike signals, and exceed it. If the intensity of the input signal is high, higher-order coherences increase in their high-frequency domains (Fig. 3b,c, last columns) and become greater than $(N-1)!/p$, indicating an essential content of combination-frequency harmonics in the response. Table 2 represents the mean values of higher-order coherences (averaged over the spectral range) of oscillations on the surface for the input signal–Gaussian noise of various intensities. The lower row shows corresponding values $(N-1)!/p$ ($p = 55$ in the calculations).

We can see from these data and from Figure 3c that if the intensity of the input Gaussian noise is high, all higher-order coherences exceed values of $(N-1)!/p$. However, calculated real and imaginary components of the higher-order coherences (Fig. 4) show that increase in the third- and fifth-order coherences is caused by the increase in scattering of their real components about a zero mean, whereas the real components of the fourth- and sixth-order coherences actually increase in the high-frequency range. Corresponding imaginary components vary about zero with zero means for any amplitudes of input and output signals. Therefore, increase in the fourth-order and sixth-order coherences indicates the cubic and the fifth-order nonlinearities of the system.

Thus, the numerical simulation shows that subsurface soils with a typical stress-strain relationship (Fig. 1a) are characterized mostly by odd types of nonlinearity, whereas even nonlinearities are weak. This is quite natural because the stress-strain curves describing the conversion of input signals into the response are described by odd functions with weak even components; in this case, even-order spectra of output signals were close to zero (Nikias and Raghuveer, 1987). For higher amplitudes of input signals, working intervals of the stress-strain curves shift to nonlinear areas, where even components gain in magnitudes. In these cases, first of all, quasi-static deformations of the surface appear as a summed effect of all even-order nonlinearities. Even-order nonlinearities are characteristic for media possessing stress-strain dependencies, which are described by functions with significant even components. For example, such behavior is observed in liquefied soils and in cases in which the stress-strain curves contain parts with large slopes (close to horizontal). In such media, additionally to quasi-static deformations, generation of even-order higher harmonics can be expected.

Table 2
Mean Values of Higher-Order Coherences of Oscillations on the Surface

Intensity of the Input Signal $\sqrt{\langle V^2(t)\rangle}$ (m/sec)	$\langle r_3^2(\omega)\rangle$	$\langle r_4^2(\omega)\rangle$	$\langle r_5^2(\omega)\rangle$	$\langle r_6^2(\omega)\rangle$
0.001	0.037	0.105	0.38	1.8
0.005	0.04	0.107	0.43	1.72
0.02	0.041	0.119	0.48	2.12
0.1	0.066	0.35	0.99	4.49
$(N-1)!/p$	0.036	0.11	0.43	2.1

Quantitative manifestations of nonlinearity, that is, amplitudes of combination-frequency harmonics, are defined by the stress-strain relationships. As is known, real stress-strain dependencies of soils obtained in experiments are very diverse and dependent on the granulometric composition of a soil, its humidity, and so on. Stress-strain curves for water-saturated soils substantially differ from the stress-strain relationship shown in Figure 1a: the initial convex-up part is followed by a deviation to the stress axis (concave-up part) (Vasil'ev *et al.,* 1977). The character of the seismic wave field and the effects of nonlinearity are different in such soils, and we can expect shock waves beyond the limit of elasticity (Zvolinskii, 1982). Stress-strain dependencies represented by the only convex-up parts are sometimes called soft diagrams (this type is characteristic for soft soils like loess loams and sands); whereas so-called "hard" dependencies composed of concave-up parts are characteristic for water-saturated sands and clays. Respectively, different indications of nonlinear behavior are known in sands and clays:

⩽

Figure 3. Changes in shapes, spectra, and higher-order coherences of seismic signals propagating in a nonlinear medium (three cases are considered, with different intensities of input signals): (a) a monochromatic signal, (b) a sum of two monochromatic signals, (c) the Gaussian noise in a wide frequency range. Row 1, input signals; row 2, the response (oscillations on the surface); row 3, power spectra of the input signals (thin lines) and spectra of the responses (thick lines); rows 4–7, one-dimensional bicoherence $r_3^2(\omega)$, tricoherence $r_4^2(\omega)$, fifth-order $r_5^2(\omega)$, and sixth-order $r_6^2(\omega)$ coherences of the input signals (thin lines) and the responses (thick lines); row 8, corresponding stress-strain diagrams (they depend on depth; maximum values are shown).

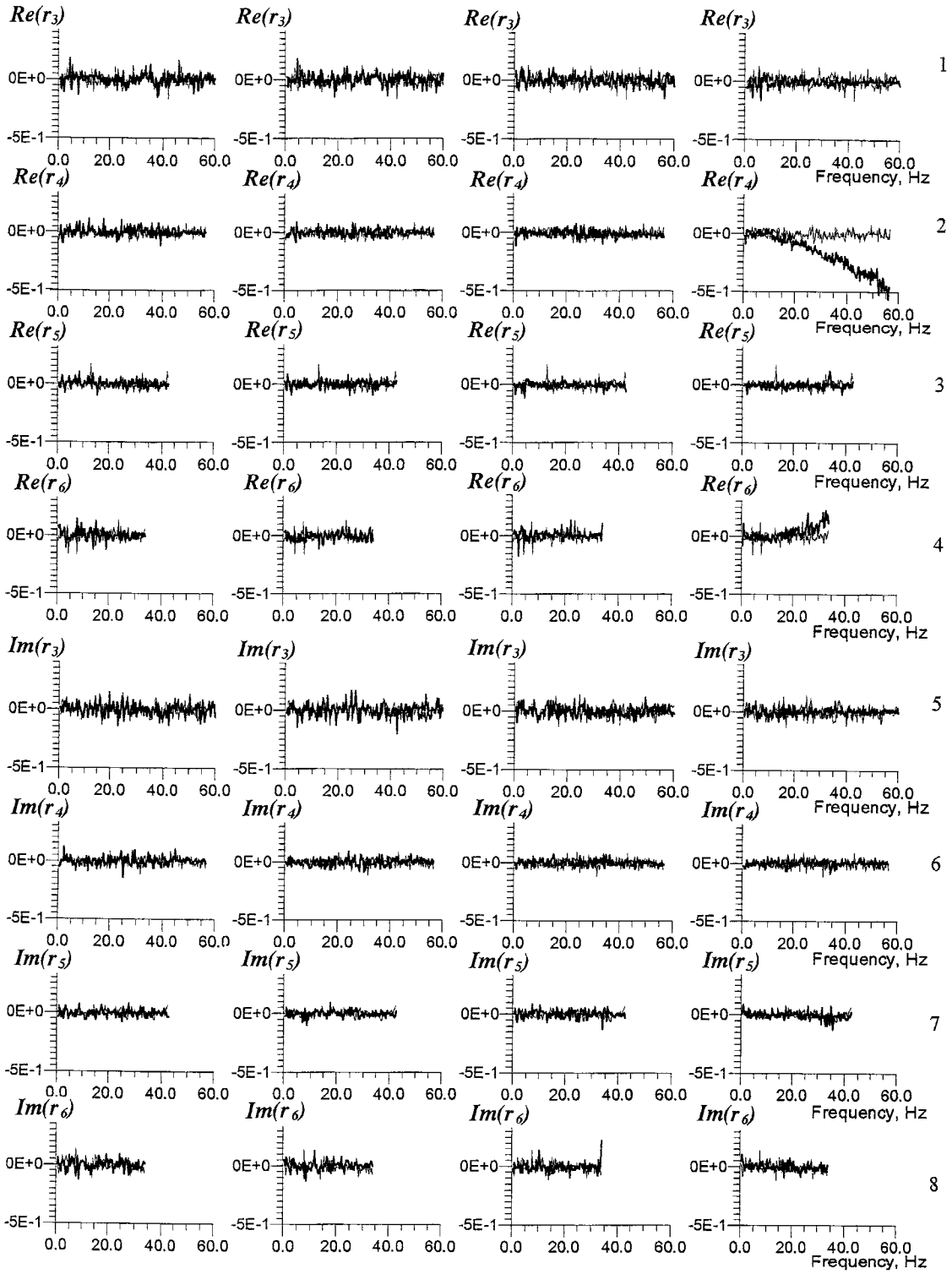

Figure 4. Real (rows 1–4) and imaginary (rows 5–8) components of higher-order coherences of the Gaussian noise in a wide frequency range: rows 1, 5, real and imaginary components of bicoherence; rows 2, 6, real and imaginary components of tricoherence; rows 3, 7, real and imaginary components of the fifth-order coherence; rows 4, 8, real and imaginary components of the sixth-order coherence. Thin lines show characteristics of input signals. Thick lines show that of output signals.

nonlinear effects are more often observed in sandy sites, whereas nonlinear behavior of clay deposits with high plasticity index appears at higher deformations (Bard, 1995).

To estimate variations in quantitative characteristics of nonlinearity for different types of soils, the calculations were repeated for cases of a more soft stress-strain relationship than that obtained by Hardin and Drnevich (1972), and for a more hard type of the relationship as well. The results were qualitatively the same: the higher harmonics of odd types were generated. For weak input signals, variations in the amplitudes of higher harmonics can achieve 200–300% depending on the model. For high amplitudes of input signals, the exponent k differs for different models.

Conclusions

Numerical simulation was performed of the propagation of vertically incident seismic waves in a system of horizontal soil layers. The method of nonlinear system identification was applied to analyze nonlinear properties of soils. Soils possessing a typical stress-strain relationship obtained in laboratory experiments by Hardin and Drnevich (1972) were studied.

The results of the numerical simulation show that nonlinear wave processes develop in soils in the following order: the third, fifth, seventh, and so on, higher harmonics of the main frequencies of the input signal are generated, and the interaction between them leads to generation of new combination-frequency harmonics. As a result, the number of spectral components increases, and the spectrum takes the form of $E(f) \sim f^{-k}$, in which k depends on dispersion, absorption, and nonlinear properties of the medium. Generation of higher harmonics was found to be more effective for higher-frequency input signals.

Therefore, in cases of weak nonlinearity (i.e., weak input signals and/or thin sedimentary layer), an increase in high-frequency components is expected, whereas in cases of strong nonlinearity (i.e., strong input signals and/or thick sedimentary layer), input signals with arbitrary spectra are transformed into output signals on the surface with spectra of the type of $E(f) \sim f^{-k}$, where k depends on the properties of the medium. A weak nonlinearity corresponds to the case in which manifestations of nonlinearity such as degradation of shear moduli and decrease in signal amplification are not noticeable, whereas, strong nonlinearity corresponds to the case in which decrease in amplification and in shear moduli can be detected.

In real media, dispersion, absorption, and seismic noise hinder the development of nonlinear processes. As a result, the third- and fifth-order nonlinearities should be of most importance in real media, whereas more higher-order nonlinearities, such as the seventh-, ninth-order are apparently negligible. The influence of even-order nonlinearities and the possibility of static deformations seem to be small in usual cases, however, they become significant in cases, when a stress-strain relationship of a soil is described by functions with noticeable even components (for example, a stress-strain dependence containing parts with slopes close to horizontal).

As a whole, nonlinear seismic processes in soils are determined by their stress-strain dependencies, by the intensity and spectral composition of the incident seismic wave, and by dispersion and absorption properties of the medium.

Acknowledgments

I wish to thank my colleagues from Radiophysical Research Institute in Nizhnii Novgorod, Vladimir V. Gushchin for his valuable comments and discussions, and Vladimir A. Shemagin for helpful recommendations concerning higher-order spectral estimation. I also thank Aleksei V. Nikolaev for his careful supervision to this research. Significant improvement to the article resulted from the comments of Arthur F. McGarr, Jonathan P. Stewart, and an anonymous reviewer. I am particularly grateful to Professor Kojiro Irikura for his encouragement and support of this work. This study was partially supported by Grants-in-Aid for Scientific Research, Number 11792026 and Number 00099 (JSPS), from the Ministry of Education, Science, Sports, and Culture of Japan.

References

Aguirre, J., and K. Irikura (1997). Nonlinearity, liquefaction, and velocity variation of soft soil layers in Port Island, Kobe, during the 1995 Hyogo-ken Nanbu earthquake, *Bull. Seism. Soc. Am.* **87,** no. 5, 1244–1258.

Aki, K., and K. Irikura (1991). Characterization and mapping of earthquake shaking for seismic zonation, in *Proc 4th Int. Conf. on Seismic Zonation,* Stanford, California, Vol. 1, 25–29, August, 61–110, EERI, Oakland, California.

Aleshin, A. S., V. V. Gushchin, M. M. Krekov, A. V. Nikolaev, and G. M. Shalashov (1981). Experimental studies of nonlinear interaction of seismic surface waves, *Dokl. Akad. Nauk SSSR,* **260,** no. 3, 574–575.

Bard, P.-Y. (1995). Effects of surface geology on ground motion: recent results and remaining issues, in *Proc. of the 10th European Conf. on Earthquake Engineering,* G. Duma (Editor), Vol. 1, Vienna, August–September 1994.

Bard, P.-Y., and K. Pitilakis (1995). Seismic zonation and ground motion interface, in *Proc. of the 5th International Conference on Seismic Zonation,* Vol. III, Nice, France, 17–19 October, Ouest Editions, Presses Academiques, Nantes, France, 2127–2152.

Beresnev, I. A., Wen K.-L., and Y. T. Yeh (1995). Nonlinear soil amplification: its corroboration in Taiwan, *Bull. Seism. Soc. Am.* **85,** 496–515.

Caillot, V., and P.-Y. Bard (1990). Characterizing site effects for earthquake regulations in the French seismicity context: a statistical analysis, in Earthquake Soil Movement; Bases and Foundations; Structure-Soil Interaction; Models of Seismic Forces Influence, *Proc. of the 9th European Conf. on Earthquake Engineering,* Vol. 4B, Moscow, 27–36.

Chang, C.-Y., C. M. Mok, and H. T. Tang (1996). Inference of dynamic shear modulus from Lotung downhole data, *J. Geotech. Eng.* **122,** no. 8, 657–665.

Darragh, R. B., and A. F. Shakal (1991). The site response of two rock and soil station pairs to strong and weak ground motion, *Bull. Seism. Soc. Am.* **81,** 1885–1899.

Dimitriu, P. P. (1990). Preliminary results of vibrator-aided experiments in nonlinear seismology conducted at Uetze, F.R.G., *Phys. Earth Planet. Interiors* **63,** 172–180.

Elgamal, A.-W., M. Zeghal, H. T. Tang, and J. C. Stepp (1995). Lotung downhole array. I: Evaluation of site dynamic properties, *J. Geotech. Eng.* **121,** no. 4, 350–362.

Groshkov, A. L., R. R. Kalimulin, G. M. Shalashov, and V. A. Shemagin (1990). Nonlinear borehole logging with the method of acoustic wave modulation by seismic fields, *Dokl. Akad. Nauk SSSR* **313,** no. 1, 63–65.

Gushchin, V. V., and G. M. Shalashov (1981). On the possibility of application of nonlinear seismic effects to problems of vibro-radiation of the earth, in *Study of the Earth by Nonexplosion Seismic Sources,* Nauka, Moscow, 144–155.

Hardin, B. O., and V. P. Drnevich (1972). Shear modulus and damping in soils: design equations and curves, *Proc. Am. Soc. Civil Eng. J. Soil Mech. Found. Div.* **98,** 667–692.

Haubrich, R. A. (1965). Earth noise, 5 to 500 millicycles per second, *J. Geophys. Res.* **70,** 1415–1427.

Joyner, W. B., and T. F. Chen (1975). Calculation of nonlinear ground response in earthquakes, *Bull. Seism. Soc. Am.* **65,** 1315–1336.

Kadomtsev, B. B., and V. I. Karpman (1971). Nonlinear waves, *Uspekhi Fiz. Nauk* **103,** no. 2, 27–48.

Kamiyama, M. (1992). Non-linear soil amplification identified empirically from strong earthquake ground motions, *J. Phys. Earth* **40,** 151–174.

Lund, F. (1983). Interpretation of the precursor to the 1960 Great Chilean Earthquake as a seismic solitary wave, *Pageoph* **121,** no. 1, 17–26.

Marmarelis, P. Z., and V. Z. Marmarelis (1978). *Analysis of Physiological Systems, The White-Noise Approach,* Plenum Press, New York.

Nikias, C. L., and M. R. Raghuveer (1987). Bispectral estimation: a digital signal processing framework, *Proc. IEEE* **75,** 869–891.

Nikolaev, A. V. (1967). Seismic properties of a loose medium, *Izv. Akad. Nauk SSSR Fiz. Zemli* **2,** 23–31.

Nikolaev, A. V. (1988). Problems of nonlinear seismology, *Phys. Earth Planet. Interiors* **50,** 1–7.

Nikolaev, A. V., O. V. Pavlenko, and A. P. Yakovlev (1995). Quasi-static vibration-induced deformations of the Earth's surface and nonlinear properties of rocks, *Physics of the Solid Earth* **30,** 1023–1030 (English translation).

Parker, D. F. (1988). Stratification effects on nonlinear elastic surface waves, *Phys. Earth Planet. Interiors* **50,** 16–25.

Vasil'ev Yu. I., L. A. Ivanova, and M. N. Shcherbo (1969). Measurement of stress and strain in a soil during the propagation of waves from explosions, *Izv. Akad. Nauk SSSR Fiz. Zemli* **1,** 21–37.

Vasil'ev Yu. I., A. A. Gvozdev, L. A. Ivanova, L. V. Molotova, V. B. Fomichev, and, M. N. Shcherbo (1977). Mechanical properties of a soft soil under stresses up to $(5–10)\cdot10^5$ Pa and selecting the model of the soil behavior in strong earthquakes, in *Seismic Microzonation,* S. V. Medvedev (Editor), Nauka, Moscow, 121–129.

Zarembo, L. K., and V. A. Krasil'nikov (1966). *Introduction to Nonlinear Acoustics,* Nauka, Moscow.

Zeghal, M., A.-W. Elgamal, H. T. Tang, and J. C. Stepp (1995). Lotung downhole array. II. Evaluation of soil nonlinear properties, *J. Geotech. Eng.* **121,** no. 4, 363–378.

Zvolinskii, N. V. (1982). Wave processes in non-elastic media, *Problems of Engineering Seismology* **23,** 4–19.

Institute of Physics of the Earth, Russian Academy of Sciences
B. Gruzinskaya 10
Moscow 123995, Russia
olga@synapse.ru

Manuscript received 31 March 2000.